Available online at www.sciencedirect.com
ScienceDirect
International Journal of Thermal Sciences 48 (2009) 655–664
International Journal of Thermal Sciences
www.elsevier.com/locate/ijts

Linear instability of mixed convection of cold water in a porous layer induced by viscous dissipation

L. Storesletten [a], A. Barletta [b,*]

[a] *Department of Mathematics, University of Agder, Serviceboks 422, 4604 Kristiansand, Norway*
[b] *Dipartimento di Ingegneria Energetica, Nucleare del Controllo Ambientale (DIENCA), Università di Bologna, Via dei Colli 16, I-40136 Bologna, Italy*

Received 12 March 2008; received in revised form 18 April 2008; accepted 19 June 2008

Available online 14 July 2008

Abstract

An analysis of linear stability of the stationary laminar Darcy flow in a horizontal porous layer is performed. The porous layer is saturated with cold water. The upper plane boundary is assumed to be subject to heat transfer with finite conductance to an environment at the temperature of maximum density of cold water. The lower plane boundary is adiabatic. Convective instabilities are caused by flow viscous dissipation, inducing a basic temperature distribution that decreases in the upward direction. For prescribed values of the Biot number Bi and the Gebhart number Ge, the critical values of the product $R = Ge\,Pe^4$, where Pe is the Péclet number associated to the basic flow solution, are determined. Disturbances in the form of oblique rolls are analyzed. It is shown that: transverse rolls are preferred at the onset of convection; critical values of R are almost independent of Ge for realistic values of this parameter; critical values of R depend on Bi and lie in an interval $36 < R < 85.6144$.

Keywords: Linear stability; Porous medium; Darcy law; Buoyant flow; Viscous dissipation; Series solution

1. Introduction

Thermally-driven convection in fluid-saturated porous media is of considerable interest and has been widely studied in the last few decades. There are important applications related both to geophysical research and to engineering problems.

A major topic of porous media research has been the problem of convection onset in horizontal layers heated from below. Detailed discussions of the literature on this subject can be found in the recent book of Nield and Bejan [1] and in the review paper by Rees [2].

In most of the studies dealing with onset of convection in horizontal layers the instability is driven by an unstable temperature gradient that is imposed externally. However, in a recent paper Barletta et al. [3] analyse the effect of viscous heating on stability. They assumed that there is no imposed temperature gradient across the layer, but rather that heat is generated internally by action of viscous dissipation. In particular the upper surface is taken to be isothermal (infinite Biot number), while the lower surface is thermally insulated. The former boundary condition is relaxed later in the paper by using a finite-Biot-number condition to represent external heat transfer to the ambient temperature.

The role played by the effect of viscous dissipation in the onset of thermally-driven instabilities of fluid flows in porous media has been disregarded in most of the literature. In fact, this effect may be very small if the temperature differences in the fluid induced by the boundary conditions are sufficiently high. This comparison between the internal heating effect of viscous dissipation and the externally prescribed temperature difference is made through a dimensionless number, i.e. the Brinkman number. Obviously, viscous dissipation plays a central role in those cases where no externally prescribed temperature difference exists in the fluid system, thus leading to an infinite Brinkman number. This condition is precisely that considered in the analysis of Barletta et al. [3]. This study is concerned with fluid having a linear relationship between density and temperature, which is standard for ordinary fluids at temperatures not too low. Convection in cold water, however, behaves in a different manner when the temperature domain encompasses

* Corresponding author.
E-mail address: antonio.barletta@mail.ing.unibo.it (A. Barletta).

1290-0729/$ – see front matter
doi:10.1016/j.ijthermalsci.2008.06.012

Nomenclature

a	nondimensional wave number, Eq. (29)
A_n	nth series coefficient, Eq. (36)
B_n	nth series coefficient, Eq. (36)
Bi	Biot number, hL/k
c_p	specific heat at constant pressure ..... $\mathrm{J\,kg^{-1}\,K^{-1}}$
c_{wave}	nondimensional phase velocity, Eq. (35)
g	modulus of gravitational acceleration ..... $\mathrm{m\,s^{-2}}$
G	nondimensional parameter, $Ge(\cos\chi)^4$
Ge	modified Gebhart number, Eq. (14)
h	external heat transfer coefficient ..... $\mathrm{W\,m^{-2}\,K^{-1}}$
K	permeability ..... $\mathrm{m^2}$
k	thermal conductivity ..... $\mathrm{W\,m^{-1}\,K^{-1}}$
L	height of the layer ..... m
n	integer number
P	nondimensional parameter, Eq. (33)
Pe	Péclet number, Eq. (17)
R	nondimensional parameter, Eq. (33)
Re	real part
$\mathbf{s}$	unit vector parallel to the base flow direction
t	nondimensional time, Eq. (8)
T	nondimensional temperature, Eq. (8)
T_m	temperature of maximum density of cold water ..... K or °C
u, v, w	nondimensional velocity components, Eq. (8)
U, V, W	nondimensional velocity disturbances, Eq. (18)
$\bar{\mathbf{u}}$	basic flow velocity ..... $\mathrm{m\,s^{-1}}$
x, y, z	nondimensional coordinates, Eq. (8)

Greek symbols

α	thermal diffusivity ..... $\mathrm{m^2\,s^{-1}}$
β^*	thermodynamic coefficient, Eq. (1) ..... $\mathrm{K^{-2}}$
β	thermal expansion coefficient ..... $\mathrm{K^{-1}}$
γ	reduced exponential coefficient, Eq. (30)
θ	nondimensional temperature disturbance, Eq. (18)
$\Theta(y)$	nondimensional function, Eq. (29)
λ	exponential coefficient, Eq. (29)
λ_1, λ_2	real and imaginary parts of λ
υ	kinematic viscosity ..... $\mathrm{m^2\,s^{-1}}$
ρ	mass density ..... $\mathrm{kg\,m^{-3}}$
ρ_m	maximum mass density of cold water .... $\mathrm{kg\,m^{-3}}$
σ	heat capacity ratio
χ	angle between the base flow direction and the x-axis
ψ	nondimensional streamfunction, Eq. (25)
$\Psi(y)$	nondimensional function, Eq. (29)

Superscript, subscripts

$-$	dimensional quantity
B	basic flow
cr	critical value

4 °C at which the density of water reaches a maximum value. In the present paper we use a quadratic density-temperature relationship. The aim is to investigate the instability of mixed convection of cold water in a porous layer induced by viscous dissipation.

There are several studies dealing with onset of thermal convection in horizontal porous layers and cavities saturated with cold water. Sun et al. [4] seem to be the first to study onset of convection of cold water using linear stability analysis. Since this work, cold water convection has received some attention. Representative papers include Blake et al. [5], Poulikakos [6], Yen [7], Mamou et al. [8] and Mahidjiba et al. [9,10]. However, none of these studies include viscous heating.

2. Governing equations

Let us consider laminar buoyant flow in a horizontal porous layer saturated with cold water. The layer is bounded above and below by two infinite and impermeable planes, separated by a distance L. The components of seepage velocity along the $\bar{x}$-, $\bar{y}$-, and $\bar{z}$-directions are denoted by $\bar{u}$, $\bar{v}$ and $\bar{w}$, respectively, where the $\bar{y}$-axis is vertical. The lower boundary wall $\bar{y}=0$ is assumed to be adiabatic, while the upper boundary wall $\bar{y}=L$ is subject to a 3rd kind thermal boundary condition representing heat transfer versus an external environment with temperature T_m, that corresponds to the maximum density of cold water.

Darcy law is assumed to be valid and the fluid density $\bar{\rho}$ varies with temperature $\bar{T}$ according to a quadratic relationship of the form

$$\bar{\rho}=\rho_m\left[1-\beta^*(\bar{T}-T_m)^2\right] \tag{1}$$

where ρ_m is the maximum density, $T_m=3.98\,^\circ\mathrm{C}$ the corresponding temperature and the coefficient $\beta^*=8\times10^{-6}\ \mathrm{K^{-2}}$. According to Moore and Weiss [11] the above relation was found to hold within 4% over the range 0–8 °C. The Oberbeck-Boussinesq approximation is applied considering T_m as the reference temperature in order to define the buoyancy contribution. Obviously, here we do not have as usual a linear equation of state, but a parabolic equation of state as shown in Eq. (1).

The governing mass, momentum and energy equations can be expressed as

$$\frac{\partial\bar{u}}{\partial\bar{x}}+\frac{\partial\bar{v}}{\partial\bar{y}}+\frac{\partial\bar{w}}{\partial\bar{z}}=0 \tag{2}$$

$$\frac{\partial\bar{v}}{\partial\bar{x}}-\frac{\partial\bar{u}}{\partial\bar{y}}=\frac{2g\beta^*K}{\upsilon}(\bar{T}-T_m)\frac{\partial\bar{T}}{\partial\bar{x}} \tag{3}$$

$$\frac{\partial\bar{v}}{\partial\bar{z}}-\frac{\partial\bar{w}}{\partial\bar{y}}=\frac{2g\beta^*K}{\upsilon}(\bar{T}-T_m)\frac{\partial\bar{T}}{\partial\bar{z}} \tag{4}$$

$$\frac{\partial\bar{u}}{\partial\bar{z}}-\frac{\partial\bar{w}}{\partial\bar{x}}=0 \tag{5}$$

$$\sigma\frac{\partial\bar{T}}{\partial\bar{t}}+\bar{u}\frac{\partial\bar{T}}{\partial\bar{x}}+\bar{v}\frac{\partial\bar{T}}{\partial\bar{y}}+\bar{w}\frac{\partial\bar{T}}{\partial\bar{z}}=\alpha\left(\frac{\partial^2\bar{T}}{\partial\bar{x}^2}+\frac{\partial^2\bar{T}}{\partial\bar{y}^2}+\frac{\partial^2\bar{T}}{\partial\bar{z}^2}\right)+\frac{\upsilon}{Kc_p}\left(\bar{u}^2+\bar{v}^2+\bar{w}^2\right) \tag{6}$$

Eqs. (3)–(5) have been obtained by applying the curl operator to both sides of Darcy law in order to encompass the dependence on the pressure field.

The velocity and temperature conditions at the lower and upper boundaries are

$$\bar{y}=0: \quad \bar{v}=0, \quad \frac{\partial \bar{T}}{\partial \bar{y}}=0$$

$$\bar{y}=L: \quad \bar{v}=0, \qquad k\frac{\partial \bar{T}}{\partial \bar{y}}+h(\bar{T}-T_m)=0 \tag{7}$$

where k is thermal conductivity and h the external heat transfer coefficient.

As described in the following sections, a forced basic flow caused by a horizontal pressure gradient is prescribed within the horizontal porous layer. The forced base flow results in a uniform basic velocity profile, with a seepage velocity of magnitude $\bar{u}_B$ at an angle χ to the x-direction, and a purely vertical heat flux.

2.1. Dimensionless formulation

Let us introduce dimensionless variables defined as

$$(\bar{x},\bar{y},\bar{z})=(x,y,z)L, \qquad \bar{t}=t\frac{\sigma L^2}{\alpha}$$

$$(\bar{u},\bar{v},\bar{w})=(u,v,w)\frac{\alpha}{L}, \qquad \bar{T}=T_m+T\frac{\upsilon\alpha}{Kc_p} \tag{8}$$

Then, the governing equations (2)–(6) can be written as

$$\frac{\partial u}{\partial x}+\frac{\partial v}{\partial y}+\frac{\partial w}{\partial z}=0 \tag{9}$$

$$\frac{\partial v}{\partial x}-\frac{\partial u}{\partial y}=2\,Ge\,T\frac{\partial T}{\partial x} \tag{10}$$

$$\frac{\partial v}{\partial z}-\frac{\partial w}{\partial y}=2\,Ge\,T\frac{\partial T}{\partial z} \tag{11}$$

$$\frac{\partial u}{\partial z}-\frac{\partial w}{\partial x}=0 \tag{12}$$

$$\frac{\partial T}{\partial t}+u\frac{\partial T}{\partial x}+v\frac{\partial T}{\partial y}+w\frac{\partial T}{\partial z}=\nabla^2 T+u^2+v^2+w^2 \tag{13}$$

where the modified Gebhart number is given by,

$$Ge=\left(\frac{g\beta^* L}{c_p}\right)\left(\frac{\upsilon\alpha}{Kc_p}\right) \tag{14}$$

The boundary conditions (7) can be rewritten as

$$y=0: \quad v=0=\frac{\partial T}{\partial y}$$

$$y=1: \quad v=0=\frac{\partial T}{\partial y}+Bi\,T \tag{15}$$

where $Bi=hL/k$ is the Biot number. The limit of a perfectly isothermal upper boundary is attained by considering $Bi\to\infty$.

2.2. Basic flow

Under these conditions there exists a uniform horizontal seepage velocity $\mathbf{u}_B=(u_B,v_B,w_B)$ in the direction of the unit vector $\mathbf{s}=(\cos\chi,0,\sin\chi)$ lying in the x,z-plane, and a purely vertical heat flux. The basic state, which we shall analyse for stability, is given by

$$u_B=Pe\cos\chi, \qquad v_B=0$$

$$w_B=Pe\sin\chi, \qquad T_B=\frac{Pe^2}{2}\left(\frac{2}{Bi}+1-y^2\right) \tag{16}$$

where Pe is the Péclet number defined by

$$Pe=\frac{(\bar{\mathbf{u}}_B\cdot\mathbf{s})L}{\alpha} \tag{17}$$

where $\bar{\mathbf{u}}_B$ is the dimensional basic flow velocity.

2.3. Linearization

Perturbations of the basic state given by Eq. (16) are given as

$$u=u_B+U, \qquad v=v_B+V$$

$$w=w_B+W, \qquad T=T_B+\theta \tag{18}$$

On substituting Eq. (18) in Eqs. (9)–(13) and neglecting nonlinear terms in the perturbations, we obtain the linearized stability equations,

$$\frac{\partial U}{\partial x}+\frac{\partial V}{\partial y}+\frac{\partial W}{\partial z}=0 \tag{19}$$

$$\frac{\partial V}{\partial x}-\frac{\partial U}{\partial y}=Ge\,Pe^2\left(1-y^2\right)\frac{\partial\theta}{\partial x} \tag{20}$$

$$\frac{\partial V}{\partial z}-\frac{\partial W}{\partial y}=Ge\,Pe^2\left(1-y^2\right)\frac{\partial\theta}{\partial z} \tag{21}$$

$$\frac{\partial U}{\partial z}-\frac{\partial W}{\partial x}=0 \tag{22}$$

$$\frac{\partial\theta}{\partial t}+Pe\cos\chi\frac{\partial\theta}{\partial x}+Pe\sin\chi\frac{\partial\theta}{\partial z}-Pe^2\,yV = \nabla^2\theta+2\,Pe\cos\chi\,U+2\,Pe\sin\chi\,W \tag{23}$$

where Eq. (16) is used. The linearity of Eqs. (19)–(23) implies that, due to the superposition property, one may treat rolls of different orientations separately with regard to instability. An advantage is that each of these cases can be dealt with using a purely 2D treatment.

3. Roll solutions of the disturbance equations

Solutions of the disturbance equations (19)–(23) are sought in the form of periodic rolls. Given that the angle χ is arbitrary, it is not restrictive to consider rolls with axes along the z-direction by first setting,

$$U=U(x,y,t), \qquad V=V(x,y,t)$$

$$W=0, \qquad \theta=\theta(x,y,t) \tag{24}$$

As a consequence, assuming $\chi = 0$ implies the analysis of transverse rolls (T-rolls) with axis orthogonal to the direction of the basic flow. On the other hand, assuming $\chi = \pi/2$ implies the study of longitudinal rolls (L-rolls) with axis parallel to the direction of the basic flow. Oblique rolls are such that $0 < \chi < \pi/2$.

Eqs. (21) and (22) are satisfied identically and, by defining a stream function ψ,

$$U = Pe^{-2}\frac{\partial \psi}{\partial y}, \qquad V = -Pe^{-2}\frac{\partial \psi}{\partial x} \tag{25}$$

also Eq. (19) is fulfilled. Moreover, Eqs. (20) and (23) can be rewritten in the form

$$\frac{\partial^2 \psi}{\partial x^2} + \frac{\partial^2 \psi}{\partial y^2} + Ge\,Pe^4\left(1 - y^2\right)\frac{\partial \theta}{\partial x} = 0 \tag{26}$$

$$\frac{\partial \theta}{\partial t} + Pe\cos\chi\,\frac{\partial \theta}{\partial x} + y\frac{\partial \psi}{\partial x} = \frac{\partial^2 \theta}{\partial x^2} + \frac{\partial^2 \theta}{\partial y^2} + 2\,Pe^{-1}\cos\chi\,\frac{\partial \psi}{\partial y} \tag{27}$$

The corresponding boundary conditions are deduced from Eqs. (15), (16), (18) and (25), namely

$$\begin{aligned} &y = 0: \quad \psi = 0 = \frac{\partial \theta}{\partial y} \\ &y = 1: \quad \psi = 0 = \frac{\partial \theta}{\partial y} + Bi\,\theta \end{aligned} \tag{28}$$

Solutions of Eqs. (26)–(28) are sought in the form of plane waves,

$$\begin{aligned} \psi(x, y, t) &= \mathrm{Re}\left\{i\Psi(y)e^{\lambda t}e^{iax}\right\} \\ \theta(x, y, t) &= \mathrm{Re}\left\{\Theta(y)e^{\lambda t}e^{iax}\right\} \end{aligned} \tag{29}$$

where the positive real constant a is the wave number, while $\lambda = \lambda_1 + i\lambda_2$ is a complex exponential growth rate to be determined. We set $\lambda_1 = 0$ in order to investigate neutral stability. Moreover, for numerical convenience we shall also set,

$$\gamma = \lambda_2 + a\,Pe\cos\chi \tag{30}$$

By substituting Eq. (29) in Eqs. (26) and (27), we obtain

$$\Psi'' - a^2\Psi + aR\left(1 - y^2\right)\Theta = 0 \tag{31}$$

$$\Theta'' - \left(i\gamma + a^2\right)\Theta + 2i\,P^{-1}\Psi' + ay\Psi = 0 \tag{32}$$

where primes denote differentiation with respect to y, and where we have introduced the nondimensional parameters

$$R = Ge\,Pe^4, \qquad P = Pe/\cos\chi \tag{33}$$

In Eq. (32), P is a modified Péclet number. In the present problem, there is not a prescribed temperature difference associated with the boundary conditions so that, strictly speaking, one cannot define a Rayleigh number. Nevertheless, since it multiplies the buoyancy term, one can consider R as a Darcy–Rayleigh number related to the characteristic temperature rise due to the viscous heating phenomenon. For the sake of brevity, in the following, R will be called Rayleigh number.

The boundary conditions for Ψ and Θ are easily deduced from Eqs. (28)–(29) to be

$$\begin{aligned} &y = 0: \quad \Psi = \Theta' = 0 \\ &y = 1: \quad \Psi = 0 = \Theta' + Bi\,\Theta \end{aligned} \tag{34}$$

The present stability analysis is based on the ordinary differential equations (31)–(32), subject to boundary conditions (34).

Eqs. (29) and (30) imply that the perturbation wave travels in the x-direction with a dimensionless phase velocity

$$c_{\mathrm{wave}} = Pe\cos\chi - \frac{\gamma}{a} = -\frac{\lambda_2}{a} \tag{35}$$

The homogeneity of Eqs. (31), (32) and (34) implies that Ψ and Θ are defined only up to an arbitrary overall scale factor, which means that we may set $\Psi'(0) = 1$ as a normalization condition. These equations form an ordinary differential eigenvalue problem with respect to R and γ, for any chosen wavenumber, a, and modified Péclet number, P. Given the definition of R in Eq. (33), this means that the critical Gebhart number may be found in terms of the Péclet number. It is more satisfactory from a physical point of view to obtain a critical Péclet number as a function of the Gebhart number but, although one may plot the variation of the Gebhart number with Péclet number, it turns out that R remains of $O(1)$ through the physically acceptable range of values of Ge.

3.1. Series solution

Eqs. (31)–(32) subject to the boundary conditions (34) may be solved by a power series method using

$$\Psi(y) = \sum_{n=0}^{\infty}\frac{A_n}{n!}y^n, \qquad \Theta(y) = \sum_{n=0}^{\infty}\frac{B_n}{n!}y^n \tag{36}$$

The three known (complex) initial conditions are

$$A_0 = \Psi(0) = 0, \qquad A_1 = \Psi'(0) = 1, \qquad B_1 = \Theta'(0) = 0 \tag{37}$$

while $B_0 = \Theta(0) \equiv \eta$ will need to be obtained by using the boundary conditions at $y = 1$, Eq. (34). Higher order coefficients A_n and B_n may be determined by substituting expressions (36) into Eqs. (31) and (32) and collecting like powers of y. We thus obtain

$$\begin{aligned} &A_2 = -aR\eta, \qquad A_3 = a^2 \\ &B_2 = \left(i\gamma + a^2\right)\eta - 2i\,P^{-1}, \qquad B_3 = 2iaRP^{-1}\eta \end{aligned} \tag{38}$$

and the recursion relations

$$\begin{aligned} A_{n+2} &= a^2 A_n - aRB_n + n(n-1)aRB_{n-2} \\ B_{n+2} &= \left(i\gamma + a^2\right)B_n - 2i\,P^{-1}A_{n+1} - naA_{n-1} \\ &n = 2, 3, 4, \ldots \end{aligned} \tag{39}$$

The series solutions given by Eqs. (36) for the neutral stability case has a rapid convergence. The real values of R and γ and the complex value of B_0 are obtained by ensuring that the two complex boundary conditions at $y = 1$ are satisfied. In all the following cases six digits of accuracy may be achieved by truncating the sum to the first 32 terms.

We also used an alternative numerical procedure based on function *NDSolve* of *Mathematica* (© Wolfram Research, Inc.).

Details are given in the following section on the stability analysis.

3.2. Stability analysis

3.2.1. Longitudinal rolls

It is important to note that, when considering L-rolls ($\chi = \pi/2$), one has $P^{-1} = 0$. In these cases, Eq. (32) loses the RP^{-1} term, and one can see that the resulting eigenvalue problem admits real eigensolutions with $\gamma = 0$. Then, for L-rolls, Eq. (35) implies $c_{\mathrm{wave}} = 0$. For each given wave number a, there exists an eigenvalue R for neutral stability independent of Ge.

The data reported in Table 1 refer to neutral stability for $Bi \to \infty$, in the case $P \to \infty$. The eigenvalues R are evaluated analytically with the power series defined by Eqs. (36)–(39), truncated to the first 32 terms, and numerically by employing function *NDSolve* within *Mathematica* environment. As shown in Table 1 there is an excellent agreement between the values of R evaluated by these two procedures.

Table 1
Comparison between the series solution and the numerical solution for $Bi \to \infty$: neutral stability data in the case of L-rolls ($\chi = \pi/2$ or $G = 0$)

a	R (series solution)	R (numerical solution)
0.1	9960.858679	9960.858679
0.2	2527.028270	2527.028270
0.4	668.9622497	668.9622497
0.6	325.4935259	325.4935259
0.8	206.0065865	206.0065865
1.0	151.4954316	151.4954316
1.2	122.7225508	122.7225508
1.4	106.2413055	106.2413055
1.6	96.43282230	96.43282231
1.8	90.61094919	90.61094920
2.0	87.35928835	87.35928838
2.2	85.87285631	85.87285637
2.4	85.66617974	85.66617985
2.6	86.43199261	86.43199281
2.8	87.96785926	87.96785960
3.0	90.13581126	90.13581182

The neutral stability curve for L-rolls, based on Table 1, is given in Fig. 1, which shows that it has the classical shape for Bénard-like problems. In this case the critical Rayleigh number and wave number are given by

$$R_{\mathrm{cr}} = 85.6144, \qquad a_{\mathrm{cr}} = 2.3362 \tag{40}$$

Fig. 2 displays the neutral stability curves for L-rolls corresponding to different values of Bi. The effect of the imperfect isothermal boundary condition at the plane $y = 1$ is an increased instability of the flow system. In fact, Fig. 2 clearly shows that, for every wave number a, the eigenvalue R is an increasing function of Bi.

3.2.2. Rolls with axes in arbitrary directions

In the general case it is suitable to introduce a parameter G related to the Gebhart number, defined by $G = Ge(\cos\chi)^4$, such that, from Eq. (33),

$$R = GP^4 \tag{41}$$

For physical reason it is convenient to use G as an ordering parameter instead of P. In fact, in judging the stability of flow in the channel, first one has to fix the channel width and the fluid properties, i.e. G. Then, one seeks the critical average velocity of the fluid above which the flow becomes unstable. In nondimensional terms, the latter step consists in evaluating the critical value of P above which the flow is unstable. To summarize, one has to fix G and then to find the critical value of P or, equivalently, of $R = GP^4$. On account of Eq. (41), for a finite non-vanishing R, the limit $P^{-1} \to 0$ coincides in fact with the limit $G \to 0$.

In the general case, the stability equations (31), (32) and (34) include five parameters, R, P, Bi, γ and a, or equivalently R, G, Bi, γ and a. For each given G, Bi and a there exist eigenvalues R and γ corresponding to neutral stability. For given G and Bi, we obtain the critical Rayleigh number R_{cr} by minimizing R with respect to the wave number a. The corresponding values for a and γ are written a_{cr} and γ_{cr}.

Table 2 shows the critical values of a, R, γ and P for different values of G, obtained by the numerical procedure based

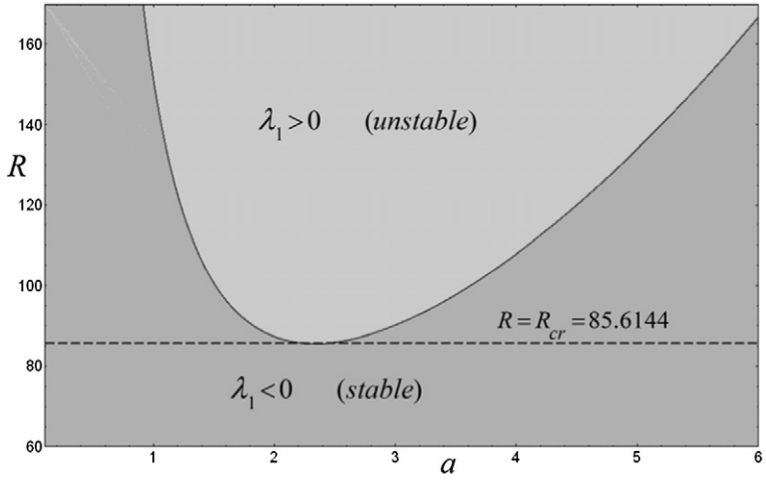

Fig. 1. Neutral stability curve for L-rolls ($G = 0$) in the case $Bi \to \infty$.

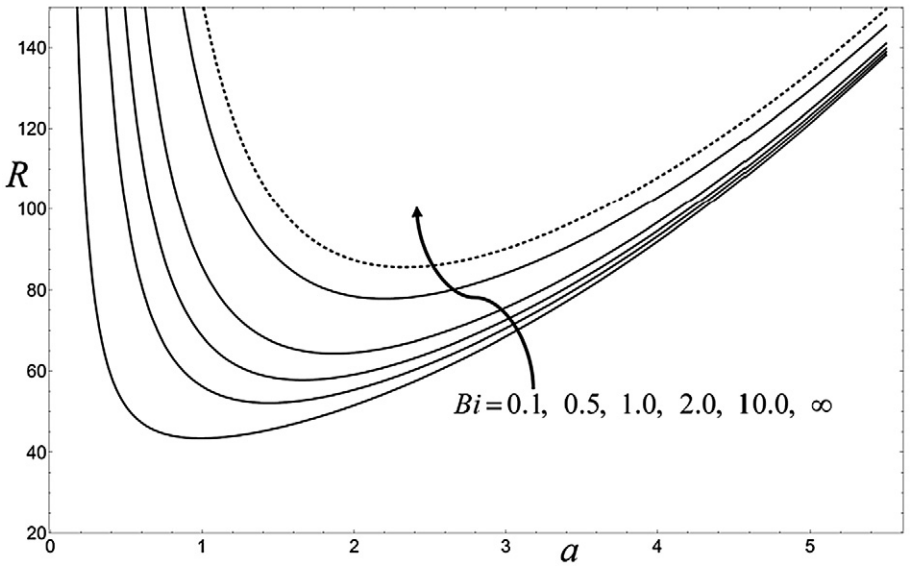

Fig. 2. Neutral stability curves for L-rolls for different *Bi*.

on function *NDSolve* of *Mathematica*. The table indicates that there is only a fairly weak variation in the critical values of R and a for small values of G, approximately $G < 10^{-8}$, which corresponds to large values of P, $P > 300$. In this regime of the parameters, the critical Rayleigh number for the onset of convection is almost independent of the roll orientation χ. The occurrence of a critical value of the Rayleigh number independent of the Gebhart number is characteristic both of the Horton–Rogers–Lapwood problem [12,13] and of Prats problem [14].

The condition $G < 10^{-8}$ defines the regime of small G where the critical values R_{cr} and a_{cr} are given with a fair approximation by Eq. (40), and one can consider approximately $\gamma_{cr} = 0$. This regime includes almost all the realistic cases. In fact, as specified in the textbook by Nield and Bejan [1], the permeability K of a porous medium is such that 10^{-16} m^2 $< K < 10^{-8}$ m^2. Then, by employing the thermodynamic data of water at atmospheric pressure reported in the textbook by Bejan [15] and by assuming $L \sim 1$ m, one can easily obtain from Eq. (14)

$$10^{-16} < Ge < 10^{-8} \tag{42}$$

Being Ge proportional to L, one can correct the range defined by Eq. (42) without difficulty, when L is higher or smaller than 1 m.

In the case $Bi \to \infty$, it is easily seen from Table 2 that rolls in the longitudinal direction, $G = 0$, have a higher critical Rayleigh number than rolls in any other direction, which means that L-rolls are the most stable. For transverse rolls ($\chi = 0$), it follows that $G = Ge$ and $P = Pe$. From Table 2 it is then seen that T-rolls are the most unstable, which implies that T-rolls are preferred at the onset of convection. These results are valid for all values of *Bi* as well.

Fig. 3 displays the respective variations of R_{cr} and a_{cr} with G, while Fig. 4 displays the variations of R_{cr} and a_{cr} with P. In these figures, the width of the small-G and large-P regime is graphically well represented. Outside this regime, one sees

Table 2
Critical values of a, R, γ, P for different G and $Bi \to \infty$

G	a_{cr}	R_{cr}	γ_{cr}	P_{cr}
0	2.3362	85.6144	0	∞
10^{-12}	2.3362	85.6144	0.0056357	3041.84
10^{-10}	2.3362	85.6142	0.017822	961.914
10^{-8}	2.3362	85.6121	0.056356	304.182
10^{-6}	2.3359	85.5910	0.17818	96.1849
10^{-5}	2.3353	85.5404	0.31671	54.0808
10^{-4}	2.3332	85.3811	0.56240	30.3977
0.001	2.3267	84.8823	0.99566	17.0688
0.005	2.3153	83.9996	1.4770	11.3848
0.01	2.3071	83.3539	1.7461	9.55502
0.05	2.2749	80.7670	2.5477	6.33966
0.1	2.2533	78.9631	2.9762	5.30098
0.5	2.1797	72.3943	4.1503	3.46883
1	2.1382	68.3437	4.7089	2.87524
1.5	2.1119	65.6231	5.0402	2.57183
2.0	2.0927	63.5454	5.2745	2.37418
5.0	2.0301	56.2442	5.9975	1.83137
10.0	1.9840	50.2544	6.5019	1.49725

from Figs. 3 and 4 that R_{cr} decreases rapidly, revealing that the flow is more likely to become unstable for very low values of P, as it is shown in Fig. 4. However, it should be remembered that instability for low values of P implies very large values of G unlikely to be displayed by a real system.

The correspondence between G and P at critical conditions is shown in Fig. 5. This figure reveals that, at critical conditions, the relation P versus G is weakly influenced by *Bi*. An approximate correlation linking G and P at critical conditions can be expressed as

$$P = 2.90358 G^{-0.253465} \quad \text{for } Bi > 10 \text{ and } 10^{-6} \leqslant G \leqslant 1 \tag{43}$$

As it is shown in Fig. 3, for G approximately lower than 10^{-4}, R_{cr} practically becomes independent of G so that, for every *Bi*, one can determine an approximate correlation linking G

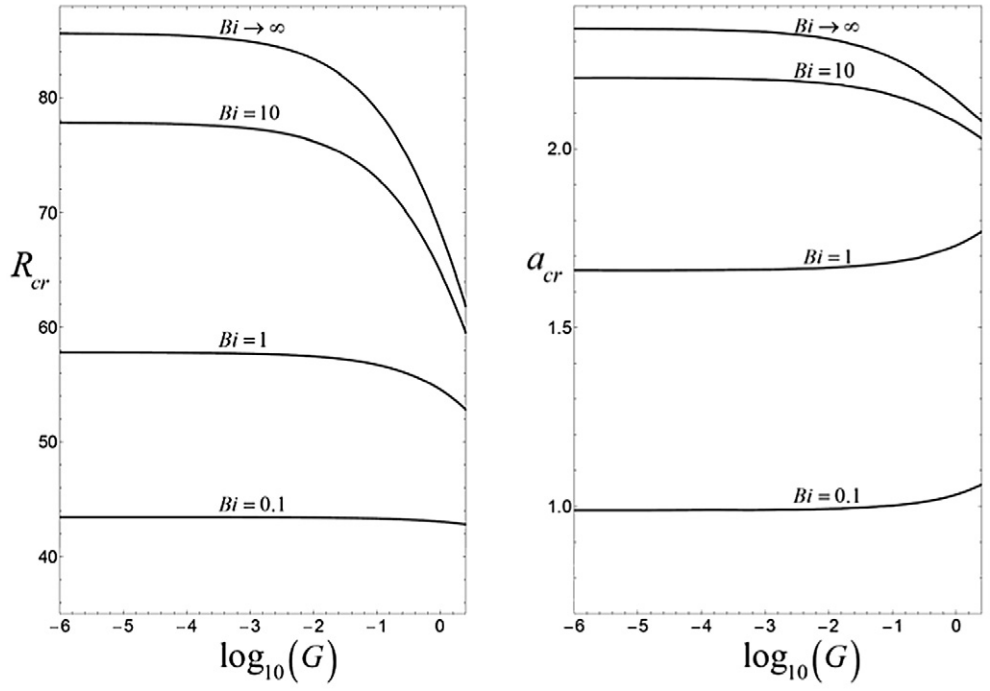

Fig. 3. Critical values of R and a versus G, for different Bi.

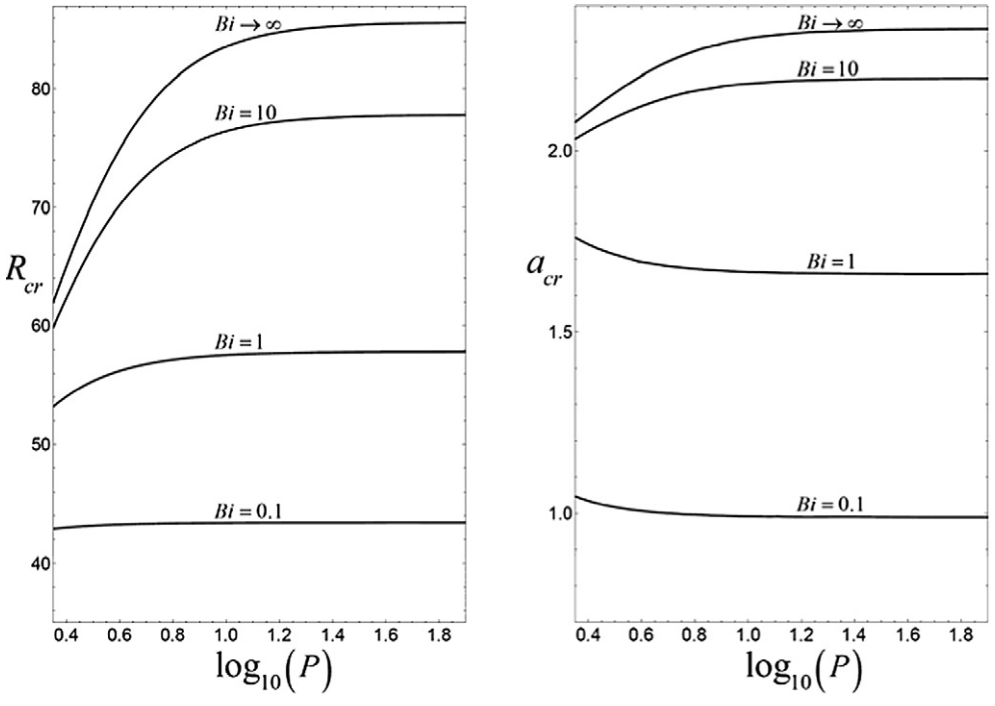

Fig. 4. Critical values of R and a versus P, for different Bi.

and P at critical conditions by employing Eq. (41) and setting, for every Bi,

$$R = \lim_{G\to 0} R_{\rm cr} \tag{44}$$

The value of $R_{\rm cr}$ in the limit $G \to 0$, that corresponds to instability for L-rolls, depends on Bi. The relation $R_{\rm cr}$ versus Bi in the limiting case $G \to 0$ is represented in Fig. 6. This figure shows that $R_{\rm cr}$ varies within the interval $36 < R_{\rm cr} < 85.6144$. The value $R_{\rm cr} = 36$ is attained for $Bi \to 0$, i.e. for the limit of upper adiabatic wall. The right frame of Fig. 6 shows that, for $Bi \to 0$, one has $a_{\rm cr} = 0$, i.e. the neutral stability curve has a monotonic increasing behavior.

Figs. 7 and 8 display streamlines and isotherms at critical conditions corresponding to the limit $G \to 0$ in two rather different cases, namely $Bi \to \infty$ (Fig. 7) and $Bi = 0.1$ (Fig. 8). The numerical values on the x-axis are not reported as the width of

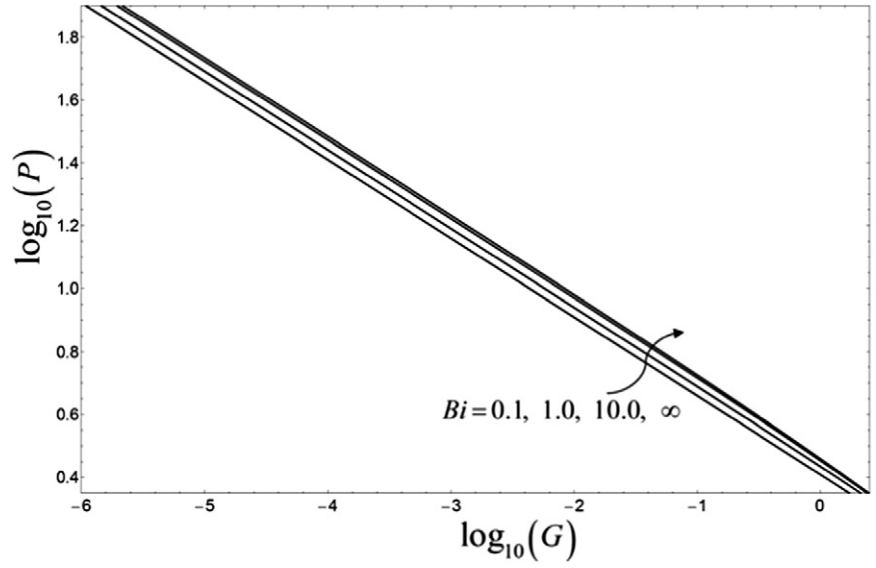

Fig. 5. P versus G relation at critical conditions, for different Bi.

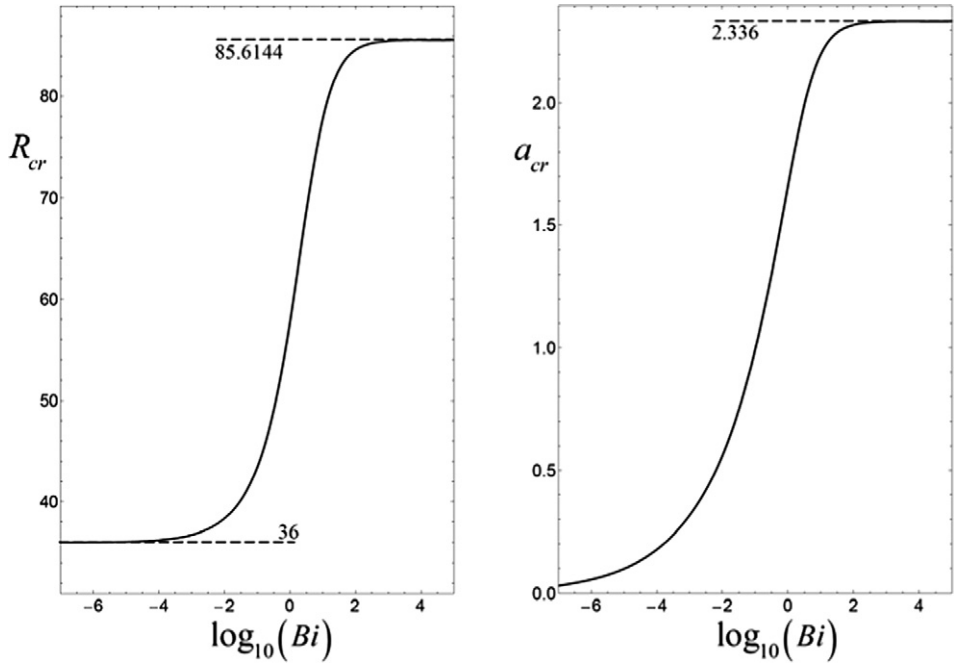

Fig. 6. Critical values of R and a versus Bi, for L-rolls ($G \to 0$).

the convection cell is determined by the critical wave number a_{cr} and, as such, changes with Bi. Moreover, only differences between values of x are physically meaningful as the solution of the disturbance equations can be arbitrarily translated along the x-axis. The most apparent difference between Figs. 7 and 8 is the shape of the isotherms describing a condition of perfectly isothermal top boundary in Fig. 7, and a condition of weak heat transfer at the top boundary in Fig. 8.

3.3. Comparison with the case of a linear equation of state

The comparison between the results obtained here with cold water and the results obtained in Ref. [3] with water in normal conditions, i.e. assuming a linear equation of state, is possible from a qualitative perspective. In fact, the set of dimensionless parameters involved in the analysis of the same problem in the case of a linear equation of state [3] includes the usual Gebhart number

$$Ge = \frac{g\beta L}{c_p} \tag{45}$$

where β is the usual thermal expansion coefficient.

On the other hand, in the present paper, the Gebhart number is in fact a modified Gebhart number given by Eq. (14), namely

$$Ge = \left(\frac{g\beta^* L}{c_p}\right)\left(\frac{\upsilon\alpha}{K c_p}\right) \tag{46}$$

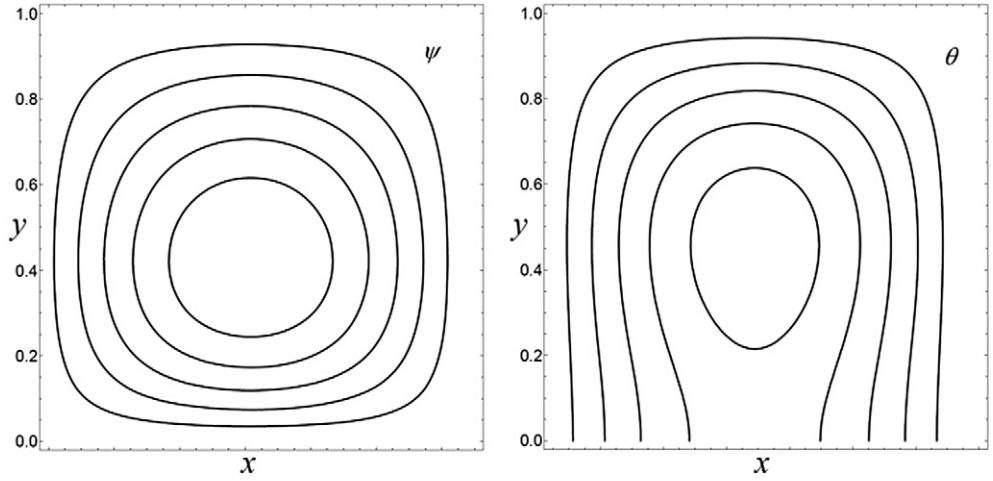

Fig. 7. Streamlines (left) and isotherms (right) corresponding to critical conditions for L-rolls ($G \to 0$) with $Bi \to \infty$.

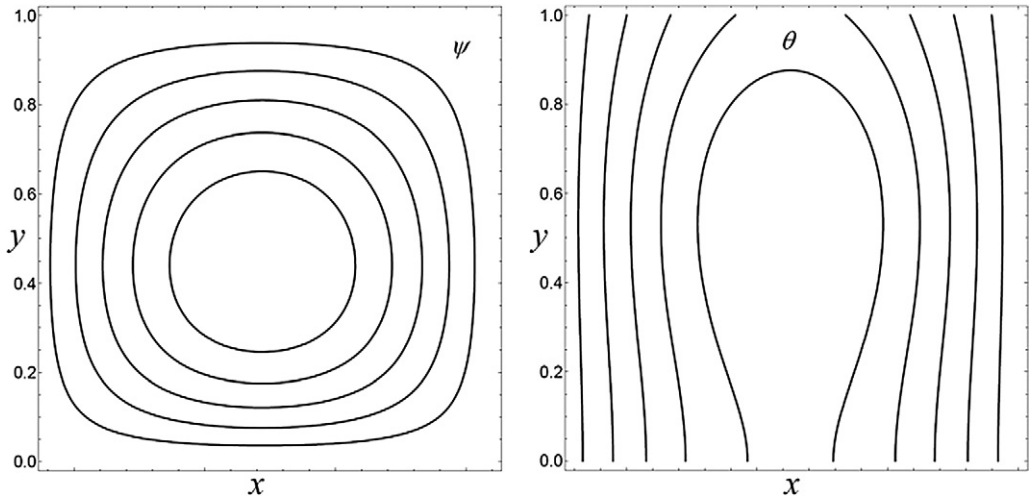

Fig. 8. Streamlines (left) and isotherms (right) corresponding to critical conditions for L-rolls ($G \to 0$) with $Bi = 0.1$.

Moreover, the driving parameter for the onset of instabilities is, in the case of water in normal conditions [3],

$$R = Ge\,Pe^2 \tag{47}$$

while, in the present case of cold water, it is, on account of Eq. (33),

$$R = Ge\,Pe^4 \tag{48}$$

The definition of Péclet number is the same in both cases, but the Gebhart number is defined differently. This leads to the main important difference between the critical conditions for the onset of convection with water in normal conditions and with cold water. In the former case, the onset of convection occurs independently of the values of permeability and fluid viscosity. In the latter case, the critical conditions for the onset of convection depend on the values of permeability and fluid viscosity.

4. Conclusions

We have considered mixed convection of cold water in a horizontal porous layer where viscous dissipation serves to raise the temperature of the moving fluid. The lower boundary of the layer is assumed to be adiabatic, while the upper boundary is subject to a 3rd kind thermal boundary condition representing heat transfer versus an external environment with temperature T_m, that corresponds to the maximum density of the cold water. The fluid density varies with temperature according to a quadratic relationship. Our aim has been to determine criteria for the onset of convection. In particular we have investigated how the instability depends on viscous heating, cold water properties and the 3rd kind boundary conditions.

In the present problem, there is no prescribed temperature difference associated with the boundary conditions so that one cannot, strictly speaking, define a Rayleigh number. Nevertheless, since it multiplies the buoyancy term, one can consider $R = Ge\,Pe^4$, where Ge is the Gebhart number and Pe the Péclet number, as a Darcy–Rayleigh number related to the characteristic temperature rise due to the viscous heating phenomenon.

Solutions of the disturbance equations are sought in the form of periodic rolls. For all Biot numbers Bi, transverse rolls turn out to be the most unstable, which implies that such rolls are preferred at onset of convection. We have found that the critical

value R_{cr} for neutral stability is approximately independent of the Gebhart number Ge in a regime including almost all physically realistic cases. In the limit of a perfectly isothermal upper boundary, $Bi \to \infty$, the critical values R_{cr} and a_{cr} are given with a fair approximation by Eq. (40) in this regime. The neutral stability curves for finite Biot numbers, given in Figs. 3 and 4, show that the critical values of both R and a reduce as Bi decreases. In the adiabatic case, $Bi \to 0$, we obtain $a_{cr} = 0$, which is consistent with the similar case for the Darcy–Bénard problem.

The relation R_{cr} versus Bi in the limiting case $G \to 0$ has been represented. It has been shown that R_{cr} varies within the interval $36 < R_{cr} < 85.6144$, where $R_{cr} = 36$ is attained for $Bi \to 0$.

References

[1] D.A. Nield, A. Bejan, Convection in Porous Media, third ed., Springer, New York, 2006.
[2] D.A.S. Rees, Stability of Darcy–Bénard convection, in: K. Vafai (Ed.), Handbook of Porous Media, Begell House, 2000, pp. 521–558.
[3] A. Barletta, M. Celli, D.A.S. Rees, The onset of convection in a porous layer induced by viscous dissipation: A linear stability analysis, Int. J. Heat Mass Transfer, 2008, in press, HMT 6598, doi:10.1016/j.ijheatmasstransfer.2008.06.001.
[4] Z.S. Sun, C. Tien, Y.C. Yen, Onset of convection in a porous medium containing liquid with a density maximum, in: Proceedings of the Fourth International Heat Transfer Conference, Paris, Versailles, NC 2 11, 1972.
[5] K.R. Blake, D. Poulikakos, A. Bejan, Natural convection near 4 °C in a water saturated porous layer heated from below, Int. J. Heat Mass Transfer 27 (1984) 2355–2363.
[6] D. Poulikakos, Onset of convection in a horizontal porous layer saturated by cold water, Int. J. Heat Mass Transfer 28 (1985) 1899–1905.
[7] Y.C. Yen, Effects of density inversion on free convective heat transfer in a porous layer heated from below, Int. J. Heat Mass Transfer 17 (1974) 1349–1356.
[8] M. Mamou, L. Robillard, P. Vasseur, Thermoconvective instability in a horizontal porous cavity saturated with cold water, Int. J. Heat Mass Transfer 42 (1999) 4487–4500.
[9] A. Mahidjiba, L. Robillard, P. Vasseur, Onset of convection in a horizontal anisotropic porous layer saturated with water near 4 °C, Int. Comm. Heat Mass Transfer 27 (2000) 765–774.
[10] A. Mahidjiba, L. Robillard, P. Vasseur, Onset of penetrative convection of cold water in a porous layer under mixed boundary conditions, Int. J. Heat Mass Transfer 49 (2006) 2820–2828.
[11] D.R. Moore, N.O. Weiss, Nonlinear penetrative convection, J. Fluid Mechan. 61 (1973) 553–581.
[12] C.W. Horton, F.T. Rogers Jr., Convection currents in a porous medium, J. Appl. Phys. 16 (1945) 367–370.
[13] E.R. Lapwood, Convection of a fluid in a porous medium, Proc. Cambridge Philos. Soc. 44 (1948) 508–521.
[14] M. Prats, The effect of horizontal fluid flow on thermally induced convection currents in porous mediums, J. Geophys. Res. 71 (1966) 4835–4838.
[15] A. Bejan, Convection Heat Transfer, Wiley, New York, 1984.